

Chemical Reactions-based Detection Mechanism for Molecular Communications

Trang Ngoc Cao, Vahid Jamali, Wayan Wicke, Phee Lep Yeoh,
Nikola Zlatanov, Jamie S Evans, and Robert Schober

Abstract—In molecular communications, the direct detection of signaling molecules may be challenging due to the lack of suitable sensors and interference from co-existing substances in the environment. Motivated by examples in nature, we investigate an indirect detection mechanism using chemical reactions between the signaling molecules and a molecular probe to produce an easy-to-measure product at the receiver. The underlying reaction-diffusion equations that describe the concentrations of the reactant and product molecules in the system are non-linear and coupled, and cannot be solved in closed-form. To analyze these molecule concentrations, we develop an efficient iterative algorithm by discretizing the time variable and solving for the space variables in each time step. We also derive insightful closed-form solutions for a special case. The accuracy of the proposed algorithm is verified by particle-based simulations. Our results show that the concentration of the product molecules has a similar characteristic over time as the concentration of the signaling molecules. We analyze the bit error rate (BER) for a threshold detector and highlight that significant improvements in the BER can be achieved by carefully choosing the molecular probe and optimizing the detection threshold.

I. INTRODUCTION

In molecular communications (MC), information is typically encoded in the number, type, or time of release of signaling molecules. The encoded information is detected at the receiver by a sensor [1]. Therefore, sensor technology, in particular chemical sensors, plays an important role for the design of receivers for MC systems.

Chemical sensors are designed to provide a measurable signal corresponding to the concentration of the analyte or the existence of a chemical substance in the environment [2]. This measurement can be based on magnetic or electrical fields, resistance, capacitance, inductance, or an optical response [2]. In MC, the selection of the sensor technique depends on the specific requirements of the considered application. For example, magnetic field based sensing was used in [3] and resistance based sensing was applied in [4]. The systems in [3] and [4] have demonstrated the possibility of realizing MC but they are fairly simple since there are no interfering sources impairing the detection of the signaling molecules, i.e., no other magnetic [3] or alcohol sources [4] besides the desired signal. Nevertheless, in many practical applications of MC, e.g., drug delivery and health monitoring, there usually exist other chemical substances which may cause interference for the detection of the signaling molecules. Environmental monitoring applications also need to handle environments where many different chemicals and electromagnetic sources are present and potentially cause interference. For example, chemicals such as zinc and copper have similar magnetic susceptibility and electrical resistivity and thus are difficult to distinguish at the

receiver. In such cases, one possible solution for detection is to harness unique chemical reactions where only the signaling molecule, i.e., the analyte, can react with a specific reactant, i.e., a molecular probe, to produce a product molecule which can be measured. This approach has been an area of intense research in molecular biology, see [2] and references therein. For example, zinc ions react with spiropyran and produce a merocyanine metal complex, which exhibits fluorescence, i.e., it emits light of a wavelength that can be measured via optical spectroscopy [2], [5]. Furthermore, synthesizing molecular probes that are matched to a given analyte and the considered environment has been an active area of research which can be exploited for MC system design, see [2] and references therein.

Note that, in some MC systems, the signaling molecules should be small and lightweight, e.g., zinc ions or calcium ions, such that they can be easily stored at the transmitter and can diffuse fast from the transmitter to the receiver. On the other hand, the product molecules of the reaction, i.e., the combination of the probe and the analyte [6], which can be detected directly by the receiver, are usually larger molecules and thus may not be directly suitable as signaling molecules. Moreover, when the reaction occurs, a measurable signal, e.g., light, corresponding to the reaction product may be generated but then disappear quickly by a process referred to as quenching [2], [7], [8], which is useful for reducing inter-symbol interference (ISI). Motivated by these advantages, in this work, we propose a novel detection mechanism for MC based on the reaction of signaling molecules with a molecular probe.

Chemical reactions have been studied in different contexts for MC. For example, chemical reactions were used to generate signaling molecules at the transmitter [9] and potent drugs on the surface of the receiver [10]. The reactions of signalling molecules with enzymes in the environment and with receptors on the surface of receivers were exploited to mitigate ISI in [11], [12] and for detection in [13]–[15], respectively. Chemical reactions have also been considered for coding and modulation in [16], [17]. In fact, in [9], the chemical reactions were assumed to occur in a one dimensional environment and the concentration of one reactant was known. The enzyme in [10] and the receptors in [13]–[15], i.e., one of the reactants, were assumed to be immobile. Moreover, [11], [12] considered a fast reaction where the concentration of the enzymes remained constant. The authors in [16], [17] focused on the concentration of the signaling molecules, i.e., the reactants, but the products of the reaction were of no interest and not studied. In [18], the molecules emitted by the transmitter and the product of

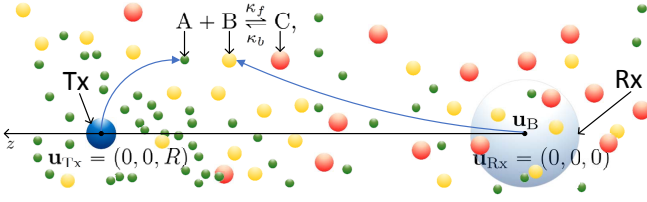


Fig. 1: Schematic illustration of the system model. A molecules are released from the transmitter, Tx, and react with B molecules, released at position \mathbf{u}_B , in order to create C molecules, which can be measured by the receiver, Rx.

the reaction during propagation were both considered, but the reaction was a degradation reaction and thus modeled as a first-order reaction. In this work, we consider the reaction between signaling molecules and molecular probes, which have to be modeled by a second-order reaction. To the best of our knowledge, second-order reactions with the reactants not being bound to the receiver and freely diffusing in the environment have not been considered for detection design of MC systems, yet. Moreover, the concentration of the reaction product in such systems, which is the solution of a second-order reaction diffusion equation, has not been analyzed.

In this paper, we consider a novel MC detection concept which is based on a chemical reaction in the environment. We make the following main contributions:

- We propose a novel detection mechanism for MC systems for which the direct detection of the signaling molecules is not possible or not efficient. A molecular probe is employed to convert the original signaling molecules into product molecules which can be efficiently detected.
- We develop an iterative algorithm for evaluation of the spatio-temporal distribution of the product molecules by solving the underlying non-linear and coupled reaction diffusion equations.
- We consider the special case where the concentration of the molecular probe is not significantly affected by the chemical reaction. This applies, e.g., when the probe is the main component of the environment and its concentration is high compared to the concentration of the analyte. For this case, we derive a closed-form expression of the concentration of the product molecules.
- We analyze the performance of the proposed detection mechanism in terms of the bit error rate (BER). Furthermore, we provide insight for system design with regard to the choice of the molecular probe and the optimal detection threshold.

II. SYSTEM MODEL AND DETECTION MECHANISM

We consider an MC system consisting of a point source transmitter, denoted by Tx, and a transparent spherical receiver, denoted by Rx, in an unbounded three dimensional (3D) diffusive environment with constant temperature and viscosity. Let R and r_{Rx} denote the distance between Tx and Rx and the radius of Rx, respectively. Using cylindrical coordinates, where position \mathbf{u} is defined as $\mathbf{u} = (\rho, \phi, z)$, $\rho \in [0, \infty)$, $\phi \in [0, 2\pi)$,

and $z = (-\infty, \infty)$, the location of Tx and Rx is given by $\mathbf{u}_{Tx} = (0, 0, R)$ and $\mathbf{u}_{Rx} = (0, 0, 0)$, respectively. Let T denote the duration of a symbol interval. We assume on-off keying modulation and that Tx releases N_A molecules of type A to convey bit “1” and no molecules to convey bit “0” at the beginning of the symbol interval, i.e., at $t = nT$, $n = 0, 1, \dots, N$, where N is the length of the bit sequence. We assume that bits “0” and “1” have equal probabilities.

We assume that the A molecules cannot be detected directly at the receiver as a suitable sensor is not available. Hence, B molecules are introduced into the system to react with the A molecules to create C molecules for which suitable sensors are available, see Fig. 1. The B molecules are referred to as molecular probes [19]. The B molecules can be released at a specific position, denoted by \mathbf{u}_B , or uniformly throughout the environment. We model the sensing process via a transparent receiver which counts the number of the C molecules in its volume without affecting the molecules. For example, for detection of the zinc ions mentioned in the introduction, optical spectroscopy is used to measure the light intensity which is proportional to the number of product molecules, i.e., the C molecules. We note that the effect of quenching, which could be exploited for ISI reduction, is neglected and left for future work. We assume that the chemical reaction between the A and B molecules is reversible and can be modeled as follows



where κ_f is the forward reaction rate constant of a second-order reaction and κ_b is the backward reaction rate constant of a first-order reaction. We assume that the A, B, and C molecules diffuse in the unbounded 3D environment with diffusion coefficients D_A , D_B , and D_C , respectively. Thereby, the concentrations of the A, B, and C molecules at time t and position \mathbf{u} , denoted by $C_i(\mathbf{u}, t)$, $i \in \{A, B, C\}$, are governed by the set of reaction diffusion equations in (2), given at the top of the next page, where ∇^2 is the Laplace operator and

$$G_i(\mathbf{u}, t) = \sum_{t_i} \sum_{\mathbf{u}_i} N_i \delta_d(t - t_i) \delta_d(\mathbf{u} - \mathbf{u}_i) \quad (3)$$

represents the concentration of the type i molecules that are released into the channel. In (3), $\delta_d(\cdot)$, N_i , t_i , and \mathbf{u}_i are the Dirac delta function, the released number molecules for each release, the release times, and the release positions of the i molecules, respectively. We note that $N_C = 0$ since the C molecules are not released. The partial differential equations (PDEs) in (2) are non-linear and coupled, i.e., the concentration of the i molecules after n releases is not equal to the sum of the concentrations originating from each release. Thus, the impact of all releases in (3) has to be accounted for when solving (2).

Let s_n and \hat{s}_n ($s_n, \hat{s}_n \in \{0, 1\}$) denote the n -th transmitted bit and the n -th detected bit, respectively. We assume threshold detection at the receiver where the receiver makes the decision on the transmitted bit based on a signal which is proportional

$$\frac{\partial C_A(\mathbf{u}, t)}{\partial t} = G_A(\mathbf{u}, t) + D_A \nabla^2 C_A(\mathbf{u}, t) - \kappa_f C_A(\mathbf{u}, t) C_B(\mathbf{u}, t) + \kappa_b C_C(\mathbf{u}, t), \quad (2a)$$

$$\frac{\partial C_B(\mathbf{u}, t)}{\partial t} = G_B(\mathbf{u}, t) + D_B \nabla^2 C_B(\mathbf{u}, t) - \kappa_f C_A(\mathbf{u}, t) C_B(\mathbf{u}, t) + \kappa_b C_C(\mathbf{u}, t), \quad (2b)$$

$$\frac{\partial C_C(\mathbf{u}, t)}{\partial t} = D_C \nabla^2 C_C(\mathbf{u}, t) + \kappa_f C_A(\mathbf{u}, t) C_B(\mathbf{u}, t) - \kappa_b C_C(\mathbf{u}, t), \quad (2c)$$

to the number of C molecules in its volume, denoted by q , at the sampling time, denoted by t_s , as follows

$$\hat{s}_n = \begin{cases} 0 & \text{if } q \leq \gamma, \\ 1 & \text{if } q > \gamma, \end{cases} \quad (4)$$

where γ is the detection threshold. We assume that the movements of the molecules are mutually independent, and thus, q approximately follows a Poisson distribution with mean \bar{q} [1]. The mean \bar{q} is given by [20]

$$\bar{q} = \int_{\mathbf{u} \in \mathcal{V}^{\text{Rx}}} C_C(\mathbf{u}, t) d\mathbf{u}, \quad (5)$$

where \mathcal{V}^{Rx} is the set of points within the receiver's volume. Note that since (2) includes the impact of all releases, $C_C(\mathbf{u}, t)$ and thus \bar{q} are affected by ISI and have different values for different sequences of n bits, denoted by $\mathbf{s}_n = [s_1, s_2, \dots, s_n]$.

The BER is given by

$$P_b = \frac{1}{2} \left(\Pr(q \leq \gamma | s_n = 1) + 1 - \Pr(q \leq \gamma | s_n = 0) \right), \quad (6)$$

where the cumulative distribution function of the Poisson distribution is given by

$$\Pr(q \leq \gamma | s_n) = \frac{1}{2^{n-1}} \sum_{\mathbf{s}_{n-1} \in \mathbb{S}} \left(\exp(-\bar{q}) \sum_{w=0}^{\gamma} \frac{\bar{q}^w}{w!} \right). \quad (7)$$

Here, \mathbb{S} is the set of all possible values of \mathbf{s}_{n-1} which affect \bar{q} .

In order to design and evaluate the system, e.g., to design γ and to calculate the BER, we need to determine $C_C(\mathbf{u}, t)$. This will be considered in the following section.

III. SYSTEM ANALYSIS FRAMEWORK

In order to design the proposed MC system and to analyze its performance, we need to obtain $C_C(\mathbf{u}, t)$. However, the non-linear coupled PDEs in (2) have no closed-form solution in general [11], [17], [21]. Thus, in this section, we first present an efficient numerical algorithm for determining $C_i(\mathbf{u}, t)$, $i \in \{A, B, C\}$, in the general case, before deriving analytical expressions for $C_i(\mathbf{u}, t)$ for a special case.

A. General Case

We adapt [17, Algorithm 1] to the problem at hand. The basic concept behind this algorithm is to discretize the time variable and to solve the PDEs in the space variable. Considering small time intervals allows us to decouple the diffusion and reaction equations¹. In particular, Algorithm 1 shown below summarizes

¹For a detailed mathematical proof of the accuracy of the algorithm with respect to the decoupling of diffusion and reaction, please refer to [17].

Algorithm 1 Iterative Calculation of the Concentration

Initialization: $t = 0, \Delta t, T^{\text{max}}$, and $C_i(\mathbf{u}, t = 0)$.

while $t \leq T^{\text{max}}$ **do**

 Update t with $t + \Delta t$.

 Compute $\bar{G}_i(\mathbf{u})$ by (10), $C_i^{\text{df}}(\mathbf{u}, t)$ by (11), and $C_i^{\text{rc}}(\mathbf{u}, t)$ by (15).

 Update $C_i(\mathbf{u}, t)$ based on (9).

end while

Return $C_i(\mathbf{u}, t)$.

the simulation steps for calculating the concentrations of the A, B, and C molecules, where T^{max} is the maximum simulation time. We will verify the accuracy of the resulting numerical algorithm via particle-based simulation in Section IV.

In Algorithm 1, $C_i(\mathbf{u}, t)$ is updated for $i = \{A, B, C\}$ in each iteration by the following rule [17]

$$C_i(\mathbf{u}, t + \Delta t) = \bar{G}_i(\mathbf{u}) + C_i^{\text{df}}(\mathbf{u}, t + \Delta t) + C_i^{\text{rc}}(\mathbf{u}, t + \Delta t) - C_i(\mathbf{u}, t), \quad (9)$$

where $\bar{G}_i(\mathbf{u})$ is the concentration of the i molecules released at \mathbf{u} in the time interval $[t, t + \Delta t]$. $C_i^{\text{df}}(\mathbf{u}, t + \Delta t)$ and $C_i^{\text{rc}}(\mathbf{u}, t + \Delta t)$ are the concentrations of the i molecules assuming that in interval $[t, t + \Delta t]$ only diffusion and only reactions occur, respectively, while the other phenomenon is absent. The updates of the concentrations in (9) are given in the following.

1) *Update of Release:* As proved in [17], $\bar{G}_i(\mathbf{u})$ is given by

$$\bar{G}_i(\mathbf{u}) = \sum_{t_i} N_i \delta_d(t + \Delta t - \epsilon - t_i) \delta_d(\mathbf{u}). \quad (10)$$

2) *Update of $C_i^{\text{df}}(\mathbf{u}, t + \Delta t)$:* As shown in [17],

$$C_i^{\text{df}}(\mathbf{u}, t + \Delta t) = \frac{1}{(4\pi D_i \Delta t)^{3/2}} \int_{\tilde{\mathbf{u}}} C_i(\tilde{\mathbf{u}}, t) \times \exp\left(-\frac{\|\mathbf{u} - \tilde{\mathbf{u}}\|^2}{4D_i \Delta t}\right) d\tilde{\mathbf{u}}. \quad (11)$$

Due to the symmetry of the system, we choose cylindrical coordinates to simplify the calculation of (11) in Corollary 1.

Corollary 1: Using cylindrical coordinates, $C_i^{\text{df}}(\mathbf{u}, t + \Delta t)$ is given by

$$C_i^{\text{df}}(\mathbf{u}, t + \Delta t) = \frac{2\pi}{(4\pi D_i \Delta t)^{3/2}} \int_{\tilde{\rho}=0}^{\infty} \int_{\tilde{z}=-\infty}^{\infty} C_i(\tilde{\rho}, \tilde{z}, t) \times W_i^z(z, \tilde{z}) W_i^\rho(\rho, \tilde{\rho}) d\tilde{z} d\tilde{\rho}, \quad (12)$$

where

$$W_i^z(z, \tilde{z}) = \exp\left(-\frac{(z - \tilde{z})^2}{4D_i\Delta t}\right), \quad (13)$$

$$W_i^\rho(\rho, \tilde{\rho}) = \exp\left(-\frac{\rho^2 - \tilde{\rho}^2}{4D_i\Delta t}\right) \tilde{\rho} I_0\left(\frac{\rho\tilde{\rho}}{2D_i\Delta t}\right), \quad (14)$$

and $I_0(\cdot)$ is the zeroth order modified Bessel function of the first kind.

Proof: Please refer to Appendix A. \square

Note that $W_i^z(z, \tilde{z})$ and $W_i^\rho(\rho, \tilde{\rho})$ do not change over time, and thus, can be evaluated offline and used online in order to reduce computational complexity.

3) *Update of $C_i^{\text{rc}}(\mathbf{u}, t)$:* Since, in this work, the product of the reaction is used for detection whereas in [17] it is of no interest for the considered system, the reaction diffusion equations in [17] are different from those in this work. Hence, in order to use Algorithm 1, we require $C_i^{\text{rc}}(\mathbf{u}, t)$, which is given in the following theorem.

Theorem 1: The concentration of the $i \in \{A, B, C\}$ molecules at time t and position \mathbf{u} assuming that only reactions occur and diffusion is absent is given by (15), given at the bottom of this page, where

$$c_{11}(\mathbf{u}) = C_A(\mathbf{u}, t) - C_B(\mathbf{u}, t), \quad (16)$$

$$c_{12}(\mathbf{u}) = C_A(\mathbf{u}, t) + C_C(\mathbf{u}, t), \quad (17)$$

$$c_2(\mathbf{u}) = \sqrt{(-\kappa_f c_{11}(\mathbf{u}) + \kappa_b)^2 + 4\kappa_f \kappa_b c_{12}(\mathbf{u})}, \quad (18)$$

$$c_3(\mathbf{u}) = C_A(\mathbf{u}, t) + C_B(\mathbf{u}, t), \quad (19)$$

$$c_4(\mathbf{u}) = \frac{c_2(\mathbf{u}) - \kappa_f c_3(\mathbf{u}) - \kappa_b}{c_2(\mathbf{u}) + \kappa_f c_3(\mathbf{u}) + \kappa_b}. \quad (20)$$

Proof: Please refer to Appendix B. \square

In some applications, the backward reaction can be very slow, i.e., $\kappa_b \rightarrow 0$. When $\kappa_b \rightarrow 0$ and $C_A(\mathbf{u}, t) = C_B(\mathbf{u}, t)$ hold, (15a) and (15b) have indeterminate forms. For this case, the $C_i^{\text{rc}}(\mathbf{u}, t + \Delta t)$ are given in the following corollary.

Corollary 2: For $\kappa_b = 0$ and $C_A(\mathbf{u}, t = 0) = C_B(\mathbf{u}, t = 0)$, we have

$$C_A^{\text{rc}}(\mathbf{u}, t + \Delta t) = C_B^{\text{rc}}(\mathbf{u}, t + \Delta t) = \frac{C_A(\mathbf{u}, t)}{1 + \kappa_f \Delta t C_A(\mathbf{u}, t)} \quad (21)$$

and $C_C^{\text{rc}}(\mathbf{u}, t + \Delta t)$ is still given by (15c).

Proof: When $\kappa_b \rightarrow 0$ and $C_A(\mathbf{u}, t) = C_B(\mathbf{u}, t)$, (21) is obtained by using L'Hospital's rule in (15a) and (15b) for $c_{11}(\mathbf{u}) \rightarrow 0$. \square

B. Special Case

In this subsection, we consider the special case when $C_B(\mathbf{u}, t)$ is very large and thus does not change significantly over time, i.e., $C_B(\mathbf{u}, t)$ is assumed to be constant over time. This assumption is similar to the assumption of uniform enzyme concentration made in [11]. The assumption is applicable when a large number of B molecules are uniformly distributed in the environment or when the B molecules have been released continuously over time from a position \mathbf{u}_B such that a steady state is reached at the beginning of information transmission. The steady state value of $C_B(\mathbf{u}, t)$ is given by

$$\begin{aligned} C_B(\mathbf{u}) &= \lim_{t \rightarrow \infty} \int_0^t C_B(\mathbf{u}, \tilde{t}) d\tilde{t} \\ &= \lim_{t \rightarrow \infty} \frac{N_B}{4\pi D_B \|\mathbf{u} - \mathbf{u}_B\|} \text{erfc}\left(\frac{\|\mathbf{u} - \mathbf{u}_B\|}{\sqrt{4D_B t}}\right) \\ &= \frac{N_B}{4\pi D_B \|\mathbf{u} - \mathbf{u}_B\|}, \end{aligned} \quad (22)$$

where $\text{erfc}(\cdot)$ is the complementary error function. Then, if $\kappa_b = 0$, and $D_A = D_C$, the closed-form expressions for $C_A(\mathbf{u}, t)$ and $C_C(\mathbf{u}, t)$ given in the following corollary are obtained.

Corollary 3: Under the above assumptions, the concentrations of the A and C molecules are given respectively by

$$C_A(\mathbf{u}, t) = \frac{N_A}{(4\pi D_A t)^{3/2}} \exp\left(-\frac{\|\mathbf{u} - \mathbf{u}_B\|^2}{4D_A t} - \kappa_f C_B(\mathbf{u}, t)t\right) \quad (23)$$

$$C_C(\mathbf{u}, t) = \frac{N_A}{(4\pi D_A t)^{3/2}} \exp\left(-\frac{\|\mathbf{u} - \mathbf{u}_B\|^2}{4D_A t}\right) - C_A(\mathbf{u}, t). \quad (24)$$

Proof: Please refer to Appendix C. \square

Remark 1: Due to (2c), $C_C(\mathbf{u}, t)$ in (24) increases fast when $C_B(\mathbf{u}, t)$ is large. For the general case, where $C_B(\mathbf{u}, t)$ reduces over time, $C_C(\mathbf{u}, t)$ given in (24) is an upper bound.

IV. SIMULATION RESULTS

In this section, we first confirm the accuracy of Algorithm 1 by particle-based simulation. We then use Algorithm 1 to analyze the concentration of the C molecules for different numbers of released B molecules. We also evaluate the system's performance in terms of the BER by Monte-Carlo simulation. For Monte-Carlo simulation, we average our results over 10^9 independent transmissions.

We simulate the system in a bounded environment using cylindrical coordinates with the limits for ρ and z large enough to approximate an unbounded environment. Let z_{\max} characterize the boundary of the environment such that $0 \leq$

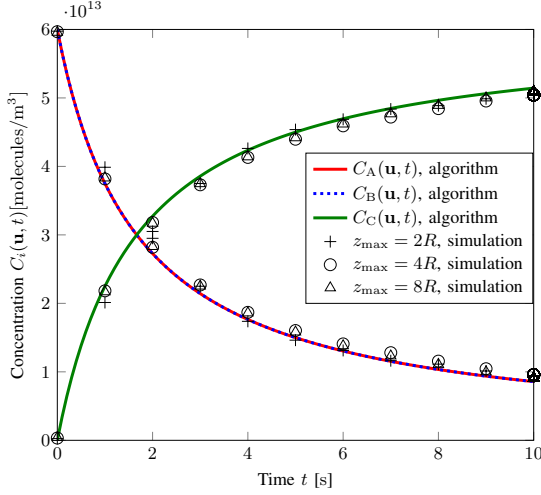
$$C_A^{\text{rc}}(\mathbf{u}, t + \Delta t) = \frac{c_2(\mathbf{u}) + \kappa_f c_{11}(\mathbf{u}) - \kappa_b - (c_2(\mathbf{u}) - \kappa_f c_{11}(\mathbf{u}) + \kappa_b) c_4(\mathbf{u}) \exp(-c_2(\mathbf{u})\Delta t)}{2\kappa_f (1 + c_4(\mathbf{u}) \exp(-c_2(\mathbf{u})\Delta t))} \quad (15a)$$

$$C_B^{\text{rc}}(\mathbf{u}, t + \Delta t) = \frac{c_2(\mathbf{u}) - \kappa_f c_{11}(\mathbf{u}) - \kappa_b - (c_2(\mathbf{u}) + \kappa_f c_{11}(\mathbf{u}) + \kappa_b) c_4(\mathbf{u}) \exp(-c_2(\mathbf{u})\Delta t)}{2\kappa_f (1 + c_4(\mathbf{u}) \exp(-c_2(\mathbf{u})\Delta t))} \quad (15b)$$

$$C_C^{\text{rc}}(\mathbf{u}, t + \Delta t) = c_{12}(\mathbf{u}) - C_A^{\text{rc}}(\mathbf{u}, t + \Delta t) \quad (15c)$$

TABLE I: System parameters used for the numerical results.

Parameter	Value	Parameter	Value
D_A [m ² /s]	10×10^{-10}	κ_f [molecules ⁻¹ · m ³ · s ⁻¹]	10^{-22}
D_C [m ² /s]	10^{-10}	κ_b [s ⁻¹]	10^{-26}
Δt [s]	10^{-2}	T [s]	10
r_{Rx} [m ³]	2.5×10^{-7}	R [m]	5×10^{-5}
N_A [molecules]	5×10^8	z_{\max} [m]	$6R = 3 \times 10^{-4}$
\mathbf{u}_{Tx} [m]	(0, 0, R)	\mathbf{u}_{Rx} [m]	(0, 0, 0)

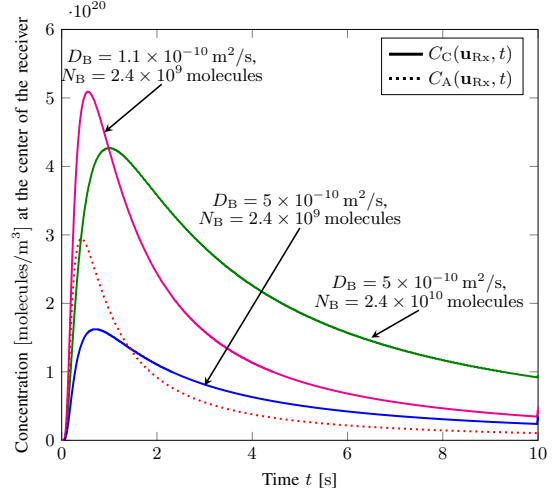

 Fig. 2: Concentrations of the A, B, and C molecules versus time, where A and B molecules are uniformly distributed in an approximately-unbounded environment limited by z_{\max} .

$\rho \leq z_{\max}$, $-z_{\max} \leq z \leq z_{\max}$. For all numerical results presented, we use the parameters provided in Table I, unless otherwise stated. For communication applications, we consider fast forward reactions, e.g., reactions with half-life time on the order of minutes or seconds. The half-life time of a reaction, denoted by $t_{1/2}$, is defined as the time for the concentration of the reactant to decrease by half of its original value [22], assuming the reactant is uniformly distributed. To select suitable parameter orders, we consider the case when the reactants are uniformly distributed and assume that the most significant change of concentration results from the forward reaction in (1), $t_{1/2} = 1$ s, and $C_A(\mathbf{u}, t) \ll C_B(\mathbf{u}, t)$ so that the A molecules can react and be converted into the C molecules without a noticeable reduction of the number of B molecules. Then, from [22, Eq. (9.14)], we have

$$\kappa_f t_{1/2} = \frac{1}{C_B^0} \ln \frac{(C_B^0 - \frac{1}{2} C_A^0) C_A^0}{\frac{1}{2} C_A^0 C_B^0} \simeq \frac{\ln 2}{C_B^0}, \quad (25)$$

where $C_i^0 = C_i(\mathbf{u}, t = 0)$. Adopting $C_B^0 = 6 \times 10^{21}$ molecules/m³ and binding constant $K_a = \kappa_f / \kappa_b = 6 \times 10^4$ molecules⁻¹ · m³ from [6], based on (25), we choose κ_f and κ_b as in Table I such that the resulting K_a has the same order as the K_a in [6].

In Fig. 2, we use the particle-based simulation described in [17, Appendix F] to confirm the accuracy of Algorithm 1, i.e., the solution of the reaction diffusion equation (2). We assume that the A, B, and C molecules are uniformly distributed with


 Fig. 3: Concentration of the A and C molecules at the center of the receiver versus time for the cases of direct and indirect detection, respectively. For the latter case, different values of D_B and N_B are considered.

$C_A(\mathbf{u}, t = 0) = C_B(\mathbf{u}, t = 0) = 6 \times 10^{13}$ molecules/m³, and $C_C(\mathbf{u}, t = 0) = 0$ molecules/m³ and have the same diffusion coefficient D_A such that diffusion does not have any impact on the concentrations of the A, B, and C molecules. In order to reduce the computational complexity for particle-based simulation, we choose $\kappa_f = 10^{-14}$ molecules⁻¹ · m³ · s⁻¹ and $\kappa_b = 10^{-18}$ s⁻¹. In Fig. 2, since the value of κ_f is larger than that of κ_b and $C_A(\mathbf{u}, t = 0) = C_B(\mathbf{u}, t = 0)$, we observe that $C_A(\mathbf{u}, t)$ and $C_B(\mathbf{u}, t)$ are equal and decrease over time while $C_C(\mathbf{u}, t)$ increases over time as expected. In general, the results obtained with Algorithm 1 are in good agreement with the simulation results. The simulation results become more accurate for larger z_{\max} , when the assumption of an unbounded environment becomes more justified.

Fig. 3 presents the concentrations of the A and C molecules at the center of the receiver versus time for the cases of direct and indirect detection, respectively. For the latter case, the B molecules are released at the center of the receiver, i.e., $\mathbf{u}_B = \mathbf{u}_{Rx}$, and we consider $D_B = 1.1 \times 10^{-10}$ m²/s, $D_B = 5 \times 10^{-10}$ m²/s and $N_B = 2.4 \times 10^9$ molecules, $N_B = 2.4 \times 10^{10}$ molecules. We observe that when the A molecules cannot be detected directly and thus the proposed indirect detection is used, the concentration of the C molecules at the center of the receiver, $C_C(\mathbf{u}_{Rx}, t)$, has a similar characteristic, i.e., a single peak and a long tail, as $C_A(\mathbf{u}_{Rx}, t)$ when the A molecules can be detected di-

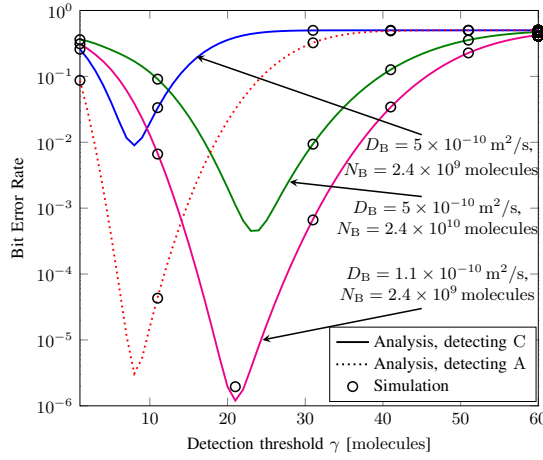


Fig. 4: BER versus detection threshold γ for direct detection via the A molecules and indirect detection via the C molecules.

rectly. Let $\max_t C_i(\mathbf{u}_{\text{Rx}}, t)$, $i \in \{A, C\}$, denote the peak of $C_i(\mathbf{u}_{\text{Rx}}, t)$, i.e., the maximum value of $C_i(\mathbf{u}_{\text{Rx}}, t)$ over time. For larger N_B and a given D_B , e.g., $D_B = 5 \times 10^{-10} \text{ m}^2/\text{s}$, the peak of $C_C(\mathbf{u}_{\text{Rx}}, t)$ is larger and can even exceed the peak of $C_A(\mathbf{u}_{\text{Rx}}, t)$. This is expected since larger amounts of the B molecules produce a larger amount of the C molecules. However, the fact that $C_C(\mathbf{u}_{\text{Rx}}, t) > C_A(\mathbf{u}_{\text{Rx}}, t)$ also means that the tail of $C_C(\mathbf{u}_{\text{Rx}}, t)$ is heavier than that of $C_A(\mathbf{u}_{\text{Rx}}, t)$. In particular, for $N_B = 2.4 \times 10^9$ molecules, although $\max_t C_C(\mathbf{u}_{\text{Rx}}, t) < \max_t C_A(\mathbf{u}_{\text{Rx}}, t)$, the tail of $C_C(\mathbf{u}_{\text{Rx}}, t)$ is heavier than that of $C_A(\mathbf{u}_{\text{Rx}}, t)$. This may negatively affect system performance due to the increased level of ISI as will be shown in Fig. 4. Nevertheless, using the C molecules for detection is unavoidable when direct detection of the A molecules is *impossible*. Similarly, for a given N_B , e.g., $N_B = 2.4 \times 10^9$ molecules, and smaller D_B , e.g., $D_B = 1.1 \times 10^{-10} \text{ m}^2/\text{s}$, the peak of $C_C(\mathbf{u}_{\text{Rx}}, t)$ is also larger since the B molecules released at the receiver diffuse away more slowly, i.e., they stay together, and can react to produce more C molecules near the receiver. However, since more reactions happen early for smaller D_B , the amount of the B molecules in the environment reduces significantly and thus less C molecules are produced at later times, which results in a lighter tail of $C_C(\mathbf{u}_{\text{Rx}}, t)$, i.e., less ISI.

Fig. 4 depicts the BER of the considered MC system versus detection threshold, γ , for the cases of direct and indirect detection. The B molecules are again released at the center of the receiver. We take the ISI caused by the previous two symbols into account, i.e., s_n is interfered by s_{n-1} and s_{n-2} , and the bit interval $T = 10 \text{ s}$ is long enough such that the contribution of other previous symbols, e.g., s_{n-3} , to the ISI is negligible. We choose the sampling time t_s equal to the time when $C_C(\mathbf{u}_{\text{Rx}}, t)$ assumes its maximum value, $\max_t C_C(\mathbf{u}_{\text{Rx}}, t)$. From Fig. 4, we observe that the analytical results obtained by (6) and (7) are in excellent agreement with corresponding Monte-Carlo simulation results. Furthermore, the BER can be reduced significantly by optimizing the detection threshold. We also observe that although $C_C(\mathbf{u}_{\text{Rx}}, t)$ for the case of

$D_B = 1.1 \times 10^{-10} \text{ m}^2/\text{s}$ and $N_B = 2.4 \times 10^9$ molecules has the highest peak in Fig. 3, the corresponding optimal detection threshold is smaller than that for the case of $D_B = 5 \times 10^{-10} \text{ m}^2/\text{s}$ and $N_B = 2.4 \times 10^{10}$ molecules. This is due to the fact that the optimal threshold depends on both the peak and the tail of $C_C(\mathbf{u}_{\text{Rx}}, t)$. Moreover, when N_B increases or D_B decreases, the optimal value of the BER decreases due to the reduced ISI. When direct detection is not available, the addition of the B molecules makes detection via the C molecules possible even if the resulting BER may be higher compared to the case when direct detection is possible. However, when the released B molecules are appropriately chosen, e.g., $D_B = 1.1 \times 10^{-10} \text{ m}^2/\text{s}$ and $N_B = 2.4 \times 10^9$ molecules, the proposed indirect detection can even achieve a lower BER than direct detection. We note that the higher BER of indirect detection for the other choices of D_B and N_B is also partly due to the suboptimal threshold detector. In the future work, we plan to consider more sophisticated detectors to further improve system performance.

V. CONCLUSIONS

In this work, we proposed a novel detection mechanism for an MC system where the signaling molecules cannot be directly detected at the receiver. Therefore, a molecular probe was introduced to react with the signaling molecules to produce product molecules that can then be detected at the receiver. We developed an efficient iterative algorithm for analyzing the spatio-temporal concentration of the product molecules taking into account diffusion and reactions. Our results showed that the concentration of the product molecules exhibits a similar characteristic over time as the concentration of the signaling molecules. We also analyzed the performance of the MC system using the proposed detection scheme in terms of the BER. Our results showed that the BER for indirect detection can be significantly improved by optimizing the detection threshold and can even be lower than the BER for direct detection if the molecular probe is suitably chosen.

APPENDIX A: PROOF OF COROLLARY 1

We can derive (12) by expanding (11) in cylindrical coordinates and substituting

$$\|\mathbf{u} - \tilde{\mathbf{u}}\|^2 = (z - \tilde{z})^2 + \rho^2 + \tilde{\rho}^2 - 2\rho\tilde{\rho}\cos(\tilde{\phi}) \quad (26)$$

into (11). Then, by using

$$\int_{\tilde{\phi}=0}^{2\pi} \exp\left(\frac{2\rho\tilde{\rho}\cos(\tilde{\phi})}{4D_i\Delta t}\right) d\tilde{\phi} = 2\pi I_0\left(\frac{\rho\tilde{\rho}}{2D_i\Delta t}\right), \quad (27)$$

we obtain (12).

APPENDIX B: PROOF OF THEOREM 1

We obtain (15) by following similar steps as in [17, Appendix D] to solve the following set of equations

$$\frac{\partial C_A^{\text{rc}}(\mathbf{u}, t)}{\partial t} = -\kappa_f C_A^{\text{rc}}(\mathbf{u}, t) C_B^{\text{rc}}(\mathbf{u}, t) + \kappa_b C_C^{\text{rc}}(\mathbf{u}, t) \quad (28a)$$

$$\frac{\partial C_B^{\text{rc}}(\mathbf{u}, t)}{\partial t} = -\kappa_f C_A^{\text{rc}}(\mathbf{u}, t) C_B^{\text{rc}}(\mathbf{u}, t) + \kappa_b C_C^{\text{rc}}(\mathbf{u}, t) \quad (28b)$$

$$\frac{\partial C_C^{\text{rc}}(\mathbf{u}, t)}{\partial t} = \kappa_f C_A^{\text{rc}}(\mathbf{u}, t) C_B^{\text{rc}}(\mathbf{u}, t) - \kappa_b C_C^{\text{rc}}(\mathbf{u}, t). \quad (28c)$$

Subtracting (28b) from (28a) and adding (28a) and (28c), respectively, we obtain

$$\frac{\partial (C_A^{\text{rc}}(\mathbf{u}, t) - C_B^{\text{rc}}(\mathbf{u}, t))}{\partial t} = 0, \quad (29)$$

$$\frac{\partial (C_A^{\text{rc}}(\mathbf{u}, t) + C_C^{\text{rc}}(\mathbf{u}, t))}{\partial t} = 0. \quad (30)$$

Equations (29) and (30) have solutions $C_A^{\text{rc}}(\mathbf{u}, t) - C_B^{\text{rc}}(\mathbf{u}, t) = c_{11}(\mathbf{u})$ and $C_A^{\text{rc}}(\mathbf{u}, t) + C_C^{\text{rc}}(\mathbf{u}, t) = c_{12}(\mathbf{u})$, where $c_{11}(\mathbf{u}) = C_A^{\text{rc}}(\mathbf{u}, t_0) - C_B^{\text{rc}}(\mathbf{u}, t_0)$ and $c_{12}(\mathbf{u}) = C_A^{\text{rc}}(\mathbf{u}, t_0) + C_C^{\text{rc}}(\mathbf{u}, t_0)$, respectively. Hence, t_0 is the initial time for which the initial conditions are known. Substituting $C_A^{\text{rc}}(\mathbf{u}, t) - C_B^{\text{rc}}(\mathbf{u}, t) = c_{11}(\mathbf{u})$ and $C_A^{\text{rc}}(\mathbf{u}, t) + C_C^{\text{rc}}(\mathbf{u}, t) = c_{12}(\mathbf{u})$ into (28a), we have

$$\begin{aligned} \frac{\partial C_A^{\text{rc}}(\mathbf{u}, t)}{\partial t} = & - \left(\kappa_f (C_A^{\text{rc}}(\mathbf{u}, t))^2 + (\kappa_f c_{11}(\mathbf{u}) + \kappa_b) \right. \\ & \left. \times C_A^{\text{rc}}(\mathbf{u}, t) - \kappa_b c_{12}(\mathbf{u}) \right), \end{aligned} \quad (31)$$

which can be written as

$$\begin{aligned} \frac{\partial (C_A^{\text{rc}}(\mathbf{u}, t))}{\kappa_f (C_A^{\text{rc}}(\mathbf{u}, t))^2 + (\kappa_f c_{11}(\mathbf{u}) + \kappa_b) C_A^{\text{rc}}(\mathbf{u}, t) - \kappa_b c_{12}(\mathbf{u})} \\ = -\partial t. \end{aligned} \quad (32)$$

Solving (32), we obtain

$$\begin{aligned} -t + \tilde{c}_4(\mathbf{u}) = \\ \frac{1}{c_2(\mathbf{u})} \ln \left(\frac{c_2(\mathbf{u}) - 2\kappa_f C_A^{\text{rc}}(\mathbf{u}, t) + \kappa_f c_{11}(\mathbf{u}) - \kappa_b}{c_2(\mathbf{u}) + 2\kappa_f C_A^{\text{rc}}(\mathbf{u}, t) - \kappa_f c_{11}(\mathbf{u}) + \kappa_b} \right), \end{aligned} \quad (33)$$

where $c_2(\mathbf{u}) = \sqrt{(-\kappa_f c_{11}(\mathbf{u}) + \kappa_b)^2 + 4\kappa_f \kappa_b c_{12}(\mathbf{u})}$ and $\tilde{c}_4(\mathbf{u})$ is a constant with respect to time. Using the initial condition when $t = 0$ in (33) leads to

$$\tilde{c}_4(\mathbf{u}) = \frac{1}{c_2(\mathbf{u})} \ln \left(\frac{c_2(\mathbf{u}) - \kappa_f c_3(\mathbf{u}) - \kappa_b}{c_2(\mathbf{u}) + \kappa_f c_3(\mathbf{u}) + \kappa_b} \right), \quad (34)$$

where $c_3(\mathbf{u}) = C_A^{\text{rc}}(\mathbf{u}, t_0) + C_B^{\text{rc}}(\mathbf{u}, t_0)$. Defining $c_4(\mathbf{u}) = \exp(c_2(\mathbf{u})\tilde{c}_4(\mathbf{u}))$, substituting (34) into (33), and setting the initial time and the current time, denoted by t_0 and t in this proof, equal to t and $\Delta t + t$, respectively, for each iteration in Algorithm 1, we obtain (15a). Using $C_B^{\text{rc}}(\mathbf{u}, t) = C_A^{\text{rc}}(\mathbf{u}, t) - c_{11}(\mathbf{u})$ and $C_C^{\text{rc}}(\mathbf{u}, t) = c_{12}(\mathbf{u}) - C_A^{\text{rc}}(\mathbf{u}, t)$, it is straightforward to obtain (15b) and (15c), respectively.

APPENDIX C: PROOF OF COROLLARY 3

The expression in (23) is obtained from [11, Eq. (9)] with $k_{-1} = 0$. Adding (2a) and (2c), we obtain

$$\frac{\partial C(\mathbf{u}, t)}{\partial t} = G_A(\mathbf{u}, t) + D_A \nabla^2 C(\mathbf{u}, t), \quad (35)$$

where $C(\mathbf{u}, t) = C_A(\mathbf{u}, t) + C_C(\mathbf{u}, t)$. From the solution $C(\mathbf{u}, t)$ of (35), we obtain (24).

REFERENCES

- [1] V. Jamali, A. Ahmadzadeh, W. Wicke, A. Noel, and R. Schober, "Channel modeling for diffusive molecular communication—A tutorial review," *Proceedings of the IEEE*, vol. 107, no. 7, pp. 1256–1301, Dec. 2019.
- [2] A. D. Johnson, R. M. Curtis, and K. J. Wallace, "Low molecular weight fluorescent probes (LMFPs) to detect the group 12 metal triad," *Chemosensors*, vol. 7, no. 2, Apr. 2019.
- [3] H. Unterwieser, J. Kirchner, W. Wicke, A. Ahmadzadeh, D. Ahmed, V. Jamali, C. Alexiou, G. Fischer, and R. Schober, "Experimental molecular communication testbed based on magnetic nanoparticles in duct flow," in *Proc. IEEE Intern. Workshop on Signal Processing Advances in Wireless Commun.*, Jun. 2018, pp. 1–5.
- [4] N. Farsad, W. Guo, and A. W. Eckford, "Tabletop molecular communication: Text messages through chemical signals," *PLOS ONE*, vol. 8, no. 12, p. e82935, Dec. 2013.
- [5] M. Natali, L. Soldi, and S. Giordani, "A photoswitchable Zn (II) selective spiropyran-based sensor," *Tetrahedron*, vol. 66, no. 38, pp. 7612–7617, Sep. 2010.
- [6] W. Luo, M. Liu, T. Yang, X. Yang, Y. Wang, and H. Xiang, "Fluorescent ZnII chemosensor mediated by a 1,8-Naphthyridine derivative and its photophysical properties," *Chemistry Open*, vol. 7, no. 8, pp. 639–644, Aug. 2018.
- [7] L. Zhao, L. Zhao, Y. Miao, C. Liu, and C. Zhang, "Construction of a turn off-on-off fluorescent system based on competitive coordination of Cu(2+) between 6,7-dihydroxycoumarin and pyrophosphate ion for sequential assay of pyrophosphatase activity," *J. of Analytical Methods in Chemistry*, vol. 2016, Sep. 2016.
- [8] X. Liu, P. Wang, J. Fu, K. Yao, K. Xue, and K. Xu, "Turn-on fluorescent sensor for Zinc and Cadmium ions based on quinolone and its sequential response to phosphate," *Journal of Luminescence*, vol. 186, pp. 16–22, Feb. 2017.
- [9] D. Bi, Y. Deng, M. Pierobon, and A. Nallanathan, "Chemical reactions-based microfluidic transmitter and receiver for molecular communication," [Online]. Available: <https://arxiv.org/pdf/1908.03441.pdf>.
- [10] U. A. K. Chude-Okonkwo, "Diffusion-controlled enzyme-catalyzed molecular communication system for targeted drug delivery," in *Proc. IEEE Global Commun. Conf.*, Dec. 2014, pp. 2826–2831.
- [11] A. Noel, K. Cheung, and R. Schober, "Improving receiver performance of diffusive molecular communication with enzymes," *IEEE Trans. Nanobiosci.*, vol. 13, no. 1, pp. 31–43, Mar. 2014.
- [12] Y. J. Cho, H. B. Yilmaz, W. Guo, and C. Chae, "Effective enzyme deployment for degradation of interference molecules in molecular communication," in *Proc. IEEE Wireless Commun. and Networking Conf.*, Mar. 2017, pp. 1–6.
- [13] H. Arjmandi, M. Zoofaghari, and A. Noel, "Diffusive molecular communication in a biological spherical environment with partially absorbing boundary," *IEEE Trans. Commun.*, vol. 67, no. 10, pp. 6858–6867, Oct. 2019.
- [14] C. T. Chou, "Extended master equation models for molecular communication networks," *IEEE Trans. Nanobiosci.*, vol. 12, no. 2, pp. 79–92, Jun. 2013.
- [15] U. A. K. Chude-Okonkwo, R. Malekian, and B. T. S. Maharaj, "Molecular communication model for targeted drug delivery in multiple disease sites with diversely expressed enzymes," *IEEE Trans. Nanobiosci.*, vol. 15, no. 3, pp. 230–245, Apr. 2016.
- [16] M. Farahnak-Ghazani, G. Aminian, M. Mirmohseni, A. Gohari, and M. Nasiri-Kenari, "On medium chemical reaction in diffusion-based molecular communication: A two-way relaying example," *IEEE Trans. Commun.*, vol. 67, no. 2, pp. 1117–1132, Feb. 2019.
- [17] V. Jamali, N. Farsad, R. Schober, and A. Goldsmith, "Diffusive molecular communications with reactive molecules: Channel modeling and signal design," *IEEE Trans. Mol. Biol. Multi-Scale Commun.*, vol. 4, no. 3, pp. 171–188, Sep. 2018.
- [18] L. Zha, Y. Deng, A. Noel, M. Elkhachan, and A. Nallanathan, in *Proc. IEEE Global Commun. Conf.*
- [19] G. Hermanson, *Bioconjugate Techniques*. UK: Academic Press, 2008.
- [20] V. Jamali, A. Ahmadzadeh, and R. Schober, "On the design of matched filters for molecule counting receivers," *IEEE Commun. Lett.*, vol. 21, no. 8, pp. 1711–1714, Aug. 2017.
- [21] L. Debnath, *Nonlinear Partial Differential Equations for Scientists and Engineers*. USA: Springer Science Business Media, 2011.
- [22] R. Chang, *Physical Chemistry for the Biosciences*. USA: University Science Books, 2005.